City Research Online

City, University of London Institutional Repository

Evaluation of different methods of determining the angle of attack on wind turbine blades under yawed inflow conditions

To cite this article: K. Vimalakanthan *et al* 2018 *J. Phys.: Conf. Ser.* **1037** 022028

View the article online for updates and enhancements.

Evaluation of different methods of determining the angle of attack on wind turbine blades under yawed inflow conditions

K. Vimalakanthan[1]**, J.G Schepers**[1]**, W.Z Shen**[2]**, H. Rahimi**[3,4]**, D. Micallef**[5]**, C.J. Simao Ferreira**[6]**, E. Jost**[7]**, L. Klein**[7]

[1] Energy Research Centre of the Netherlands (ECN), 1755 LE Petten, The Netherlands
[2] Department of Wind Energy, Technical University of Denmark, Lyngby, Denmark
[3] ForWind, Institute of Physics, University of Oldenburg, Oldenburg, Germany
[4] Fraunhofer Institute for Wind Energy Systems (IWES), Oldenburg, Germany
[5] Department of Environmental Design, University of Malta, Msida, Malta
[6] Department of Wind Energy, Delft University of Technology, Delft, Netherlands
[7] Institute of Aerodynamics and Gas Dynamics, University of Stuttgart, Stuttgart, Germany

E-mail: `kisorthman.vimalakanthan@tno.nl, gerard.schepers@tno.nl`

Abstract. As part of the AVATAR and Mexnext projects, this study compares several methods used to derive lifting line variables from CFD simulations of the MEXICO rotor in yawed inflow. The results from six partners within the AVATAR/Mexnext consortium using five different methods of extraction were compared. Overall comparison of the induced velocities at the mid and tip parts of blade shows fairly good agreement between the tested methods, where the derived angle of attack differs within $1°$, within the linear range this accounts to $<10\%$ uncertainty on the aerodynamic forces. The presented comparison shows inadequate agreement between the methods for application towards the root.

1. Introduction

The calculation of a wind turbine design load spectrum is very time consuming [1] and requires the application of a low fidelity aerodynamic model based on the blade element momentum(BEM) method. In these methods the rotor blades are modeled in a simplified way through lifting lines approaches. A common procedure to improve the accuracy of such low fidelity methods is to calibrate them with results from high fidelity CFD calculations or experiments in which the rotor blades are fully resolved. However the verification of lifting line parameters like the angle of attack (AoA) and the induced velocity is difficult because these parameters are based on hypothetical quantities such as induced velocities where CFD provides "real" physical flow field data. Several methods have been invented which translate CFD results into lifting line parameters but the accuracy of these methods is unknown. Therefore within a joint effort of the EU project AVATAR and IEA Task 29 Mexnext, a benchmark was organised which compares the results from a large number of methods available to the participants using the same CFD results as a basis. In [2] the results from this benchmark for axi-symmetric conditions with the methods used for this work are described, and the present paper describes the results achieved for the MEXICO rotor under yawed conditions. The CFD results to be used

were provided by DTU, where DTU-Ellipsys 3D solver was used to perform steady simulations of MEXICO rotor at 30° yawed inflow, at various rotor azimutal positions (0°:30°:330°).

Yawed wind turbines have been studied extensively in the past (see for instance [3], [4], [5], [6], [7] [8]). Focused research on this topic is required mainly due to the quite common occurrence when the turbine rotor is not aligned with the wind direction. Lately this has led to a number of efforts directed at understanding the flow physics in the case of yawed flow. Such experiments include those carried out under the Model Experiments Under Controlled Conditions (MEXICO) [9] and also those performed by Maeda et al. [10] and Micallef [11]. A complete review of yawed wind turbine aerodynamics is given in [12].

The AoA in the case of yawed turbine becomes dependent on the azimuth angle of the blade due to the in plane component of the free-stream velocity. This will influence the blade loads and how they vary with the azimuthal position ([13], [14]). As opposed to the axi-symmetric flow case, there is also an additional complexity that when the blades are in their horizontal position, the in-plane component of the free-stream causes an outboard or an inboard flow which makes the flow highly three-dimensional for these positions. This notion goes against the pre-established idea that the AoA is fundamentally speaking a two-dimensional quantity, that neglects boundary layer development via three-dimensional flow field. The results of Rahimi et al. [2] show how the various methods for calculating the AoA can be successful for 2D predominant mid-board flows but have shown discrepancies in the methods in the 3D dominated flows such as the tip. Whether the yawed case presents new challenges even for the mid-board sections at various azimuth angles remains to be unraveled.

This study compares the results from six partners within the AVATAR/Mexnext consortium using five different methods of extractions. Implementations of these methods were carried out by Energy Research Centre of the Netherlands (ECN), University of Stuttgart (USTUTT), Delft University of Technology/University of Malta (Delft/Malta) and ForWind-University of Oldenburg/Fraunhofer IWES (FW/IWES).

2. CFD simulations
The CFD results to be studied were provided by DTU, where DTU-Ellipsys solver [15][16][17] was used to perform steady simulations of Mexico rotor at 30° yawed inflow. Simulation were performed at the following conditions: Wind speed = 15.01 m/s and Rotor speed= 425.1 rpm, Rotor pitch= -2.3°. The rotor azimuthal position was tested with 30° step i.e. Azimuthal position = 0:30:330. The Mexico turbine is a three bladed rotor with a diameter of 4.5m, including a speed controller and pitch actuator. It is a bespoke design for the MEXICO wind tunnel measurement campaign with a design tip speed ratio of 6.7. For more details on the rotor and the experimental setup, see [18].

3. Lifting line variable extraction methods
Several methods have been developed to extract lifting line variables from CFD and experimental flow field data, this section provides a brief description of the methods used within this study.

The Shen et al's Upwash methods models the blade as a concentrated circulation line [19] or as a bound vorticity distribution [20] based on the local pressure distribution. These methods are denoted by Upwash1 and Upwash2, respectively. In Upwash1, the AoA is determined by (1) estimating the lift force by projecting the force along the incoming and normal to the incoming directions; (2) calculating the bound vortex using the Kutta-Joukowski law; (3) calculating the induced velocity by the bound vortex using Biot-Savart's law; (4) computing the relative velocity at the monitor points by subtracting the induced velocity from the bound vortex; (5) computing the AoA from the relative velocity. This procedure continues until the convergence is reached. The position of the monitoring/probing point is important for this method as the bound vortex is considered as a line vortex along the blade. The points cannot be chosen too close to the blade
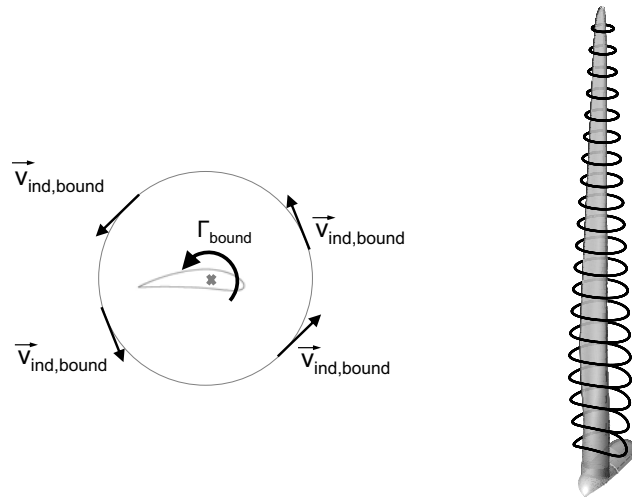
Figure 1. Schematic of the Line Average approach used here [21].

since this causes a singularity problem and the induced velocity approaches infinite. Therefore it is suggested that the monitoring point location be 2*chord away from the leading-edge in the rotational plane.

In order to overcome the difficulty of singularity in the Upwash1 method, an alternative technique was presented in [20], where a distributed bound circulation along the airfoil/blade surface is used instead of the concentrated bound vortex at the force center. In this case, the monitor points can be chosen closer to the blade and it is shown that for this method the results are not depending on the location of monitoring points. It is suggested that the monitoring point location to be chosen from .5*chord away from the leading-edge in the rotational plane. Another advantage is that this method takes the chordwise variation of aerodynamic forces into account which is neglected when the vorticity is concentrated in a bound vortex. Additionally, this method is not iterative. However, the difficulty of using this method is to find the separation point (SP) where the local circulation changes sign. For this benchmark study: 3*chord lengths from the leading edge of the section of interest along its respective radial position are chosen for both Upwash methods.

The Line Average method (LineAve) studied in [21] was also included in this benchmark study, where the velocity around a point-symmetric closed line centered at the quarter chord of the respective radial section is averaged to eliminate the effect of the bound circulation, thus providing the local inflow vectors. The method was found especially valuable in the outer and tip area of the blade due the very local approach. In the present case, a circle with a radius equal to the local chord length was used (Figure 1). The circle center is placed at the quarter chord position, where like in a lifting line representation the bound vortex is located. The idea is that the induced velocities at opposed points on the circle extinguish each other. By averaging the flow velocities along the circle, the influence of bound circulation is eliminated and the local inflow velocity and AoA can be determined. The local circle radius is varied along the blade span and chosen dependent on the local chord length c. For this benchmark study, $r_{circ} = 3c$ is used.

A method based on an inverse vortex approach was included in this benchmark (FERREIRA-MICALLEF). This method is based on an inverse potential flow vortex approach wherein the experimental or high fidelity numerically calculated velocities are used as the solution to a 2D vortex approach where the flow field is discretised into a number of free vortices. The velocities
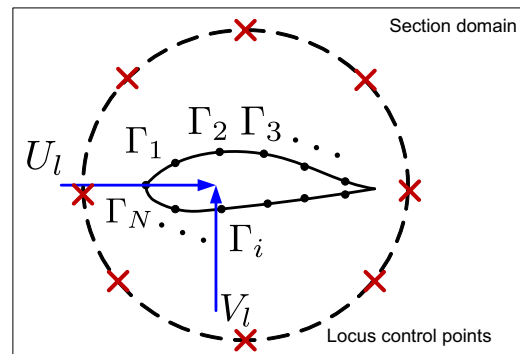
Figure 2. Schematic of the inverse vortex approach used here.

can be attributed to three main components: (1) the local wind velocity, (2) the free vortices in the vicinity of the blade and (3) the bound vortices. A locus of points around the airfoil is used. At these points the resulting flow field is known from the data available. The bound circulations on the blade and local velocities in the horizontal and vertical directions (U_l and V_l respectively) can be found as the unknowns of the problem. A schematic is shown in fig. 2. The velocities at the locus of control points at (x, y) by a point vortex located at (x_ω, y_ω) are given by Equations 1 and 2, where u_ω is the velocity induced in x-direction and v_ω is the velocity induced in y-direction.

$$u_\omega = \frac{\Gamma}{2\pi} \frac{y - y_\omega}{(x - x_\omega)^2 + (y - y_\omega)^2} \tag{1}$$

$$v_\omega = -\frac{\Gamma}{2\pi} \frac{x - x_\omega}{(x - x_\omega)^2 + (y - y_\omega)^2} \tag{2}$$

A linear over-constrained system can be written which involves the unknown bound circulations Γ_i and the local velocities for the section (U_l, V_l). To solve such a system, the linear least squares approach needs to be be used. The found (U_l, V_l) can then be used to determine the AoA:

$$\alpha = \tan^{-1}\left(\frac{V_l}{U_l}\right) \tag{3}$$

Additionally, the 3−Point method introduced by Rahimi et al [22, 2] denoted with 3P was also tested in this benchmark study. This method is based on the average azimuthal technique (AAT) [23][24], however it uses only three points along the chord length on each side of the blade section to perform the averaging of the velocities and extract the AoA (Figure 3). This great simplicity is the main advantage of this method, which makes the calculation of the AoA very straightforward. By choosing three points at each section, the influence of bound circulation as well as the upwash and downwash effect is eliminated. In addition, unlike the AAT method, this method is able to reproduce the dynamic behavior of the induction and AoA (local induced velocity and AoA) for each azimuthal position and also near the tip and root of the blade which is very important for the yawed flow. This has been shown in previous works with a comparison to a lifting line free vortex wake code [22].

For this method, three points on each side of a particular section which is modeled as an airfoil will be assigned. These points are located at 25, 50 and 75 % of chord length along the airfoil at both sides. The idea is that these points cancel out the effect of the bound vortex
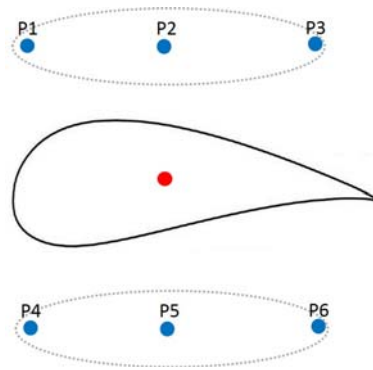
Figure 3. Schematic of the 3-Point approach used here

and reduce the effect of flow separation on the resulting induced velocity. The procedure of extracting the induced velocity is as following: (1) For each pair of points (at upstream and downstream locations) (P1,P4), (P2,P5) and (P3, P6) the velocity are averaged independently by using an interpolation function. The three velocity $V_{1,4}$, $V_{2,5}$, $V_{3,6}$ are therefore obtained. (2) The estimated velocity which is induced at the blade section (red point) at the airfoil center can be easily found by simple averaging as: $V_{averaged} = (V_{1,4} + V_{2,5} + V_{3,6})/3$. (3) By knowing the induced velocity at the rotor plane, and the blade twist, the AoA for a given radial location can be found by:

$$\alpha = tan^{-1} \left(\frac{V_{averaged}}{r\Omega} \right) - \varepsilon \tag{4}$$

One shortcoming of this method could be that the solution may be dependent of the 3 points locations near the very root (up to 10% blade length) and tip (from 90% blade length) where the flow is 3D[25]. For these spanwise positions, other methods, like e.g. Upwash2 are preferred.

4. Results
The induced velocities (Uind) and the corresponding AoA at three spanwise locations namely: r=0.45m (20%R), 1.125m (50%R) and 2.025m (90%R) for blade1 were compared along the azimuth for all the above mentioned methods. Based on the computed AoA, the corresponding aerodynamic coefficients (lift:Cl and drag:Cd) from 2D sectional data, which are generally used for BEM calculations are compared between all methods.

4.1. Root: 20%R
Comparing the results at the root part of the blade (Figure 6), shows large differences between the different methods. This was also observed for axial flow conditions in [2]. It also shows poor agreement between the trends in induced velocities along the azimuth. The ECN and USTUTT implementation of the Upwash1 method shows good agreement up to 180° azimuth. The Upwash methods (Upwash1 and Upwash2) shows similar trends in induced velocity. The largest scatter is seen at the azimuth angle between 30-180° (σ_{Uind}=0.9m/s).

Due to the large differences in AoA ($>10°$), the overall comparison of the forces (Figure 7) computes up to 12% differences in lift forces, while much larger differences up to 70% is seen for the drag forces. Despite the torque production from this part of the blade being insensitive to drag forces [25], and the structural integrity of the root may accommodate the thrust loadings from drag uncertainties, the 70% differences in drag forces leaves the tested methods inadequate for extracting induced velocities from yawed flow at root part of the blade. In combination with the root vortex, the highly three dimensional nature of the root flow seems to violate the 2D
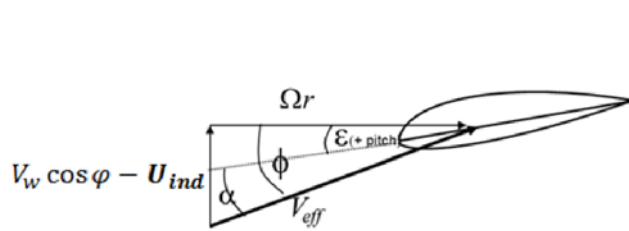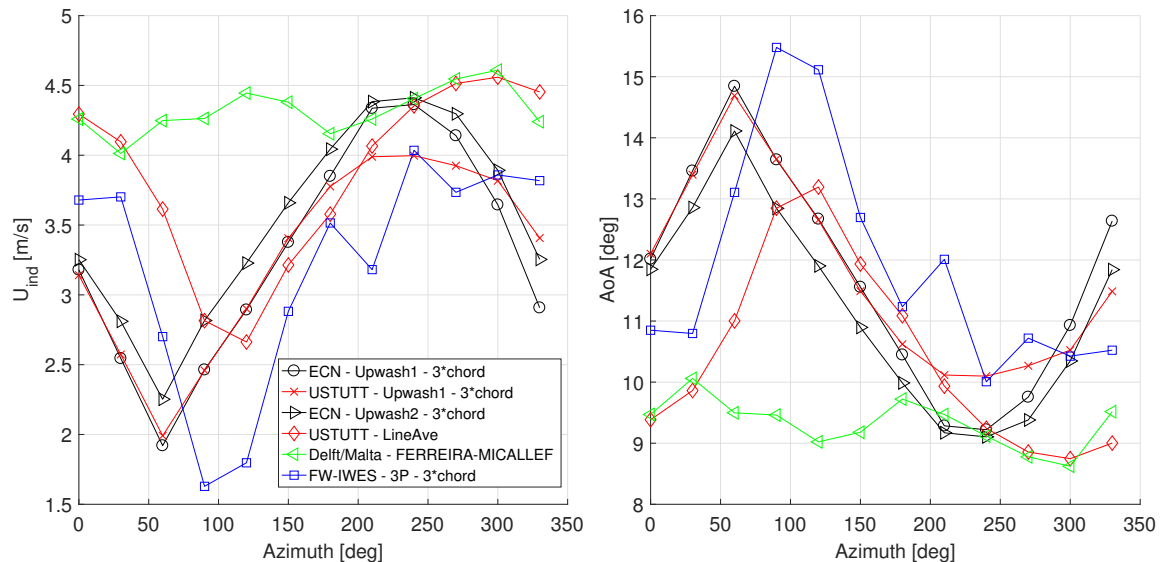
Figure 4. Wind turbine velocity triangle showing the benchmarking quantity (Uind), where V_w= wind speed, φ= yaw angle, Ω=Rotational speed, α=AoA, ϕ= relative flow angle and ϵ= sectional twist angle
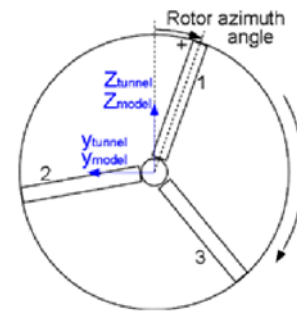
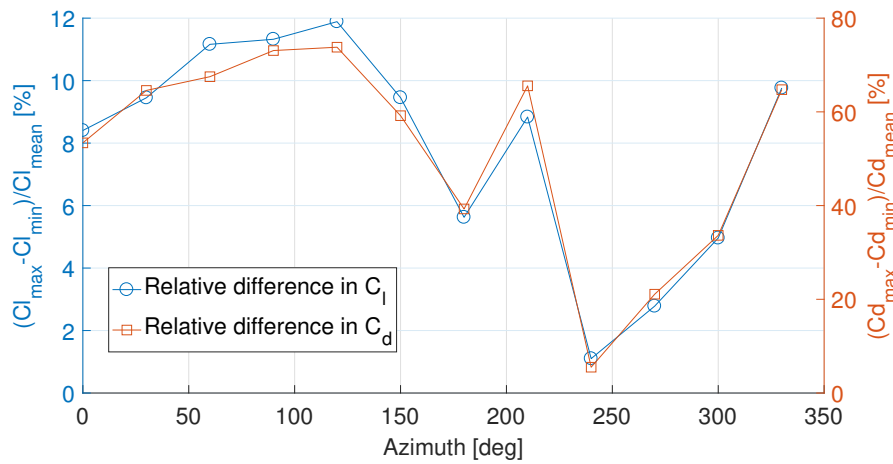**Figure 5.** Rotor azimuth direction and blade numbers [18]

Figure 6. Azimuthal variation of induced velocity (left) and AoA (right) at 20% blade span, MEXICO rotor, Wind speed = 15m/s with 30° yaw

circulation assumption. Specifically the Upwash methods rely on the pressure distribution being established by the 2D flow, while within the hub separation a strong radial flow significantly influences the local pressure distribution [25].

4.2. Mid-span: 50%R
Better agreement is achieved at the mid part of the blade, where the 2D flow assumption are consistent with the local flow characteristics. Quantifying the scatter between all methods shows that the largest standard deviation of σ_{Uind}=0.23m/s is found to accumulate around the azimuth angle of 210°. The derived AoA from all other methods differ within 1° at this mid part of the blade. This result in <8% differences in sectional lift forces and <4% for the drag forces (Figure 9), which makes all methods better suited for this part of the blade, for extracting induced

Figure 7. Relative differences in BEM force coefficients between all methods at 20% blade span
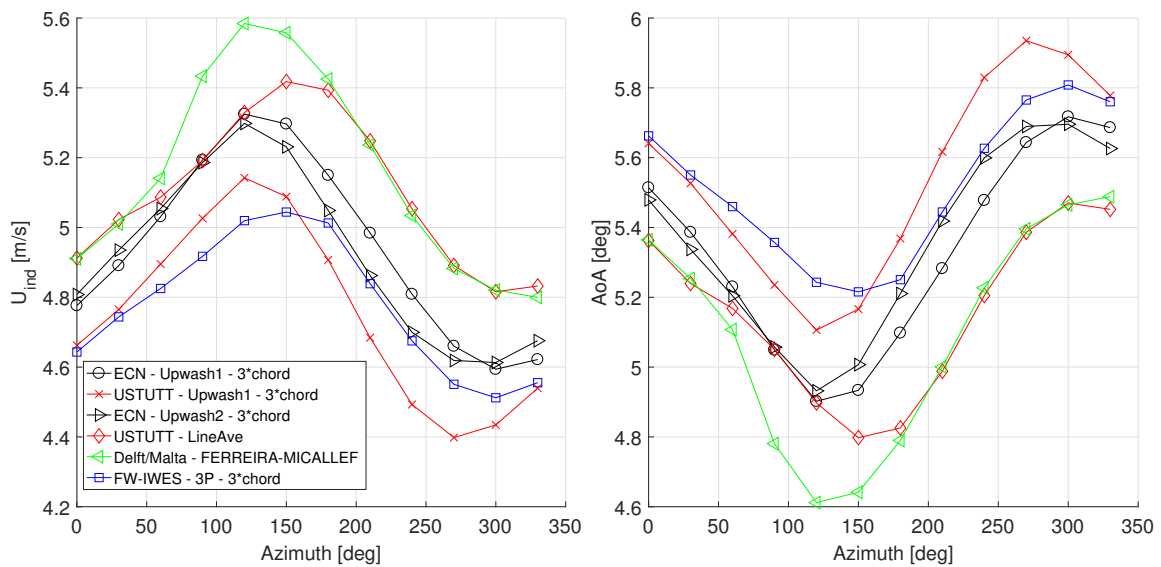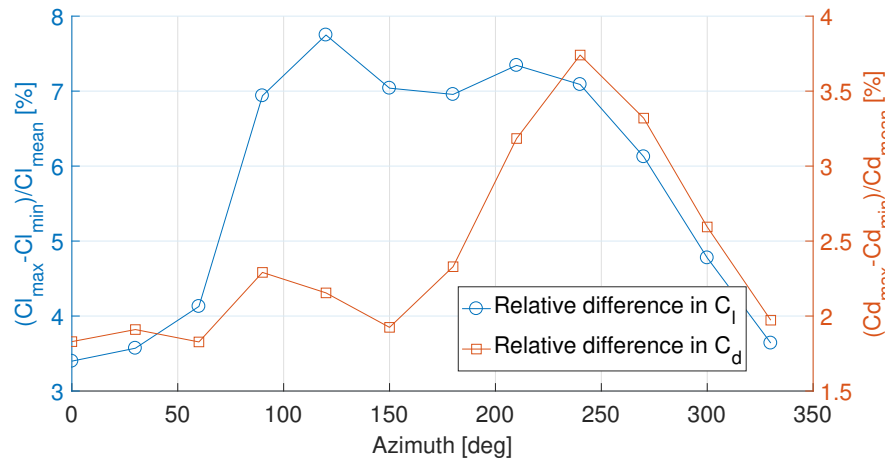

Figure 8. Azimuthal variation of induced velocity (left) and AoA right) at 50% blade span, Mexico rotor, Wind speed = 15m/s with 30° yaw

velocities with comparable confidence. The lower drag differences are also attributed to the operating AoA are in the linear region along its entire azimuth.

4.3. Tip: 90%R

At this part of the blade the scatter between the methods once again seems to increase (σ_{Uind}=0.5m/s at Azimuth=240°) due to expected influence of the tip vortex (Figures 10 and 11). However, contrary to the results found at the root part of the blade, better agreement is achieved on the trends. The derived AoA from all methods are again established within 1° at this tip parts of the blade, however the 18% t/c section at this part of the blade has a drag rise AoA

Figure 9. Relative differences in BEM force coefficients between all methods at 50% blade span

Figure 10. Azimuthal variation of induced velocity (left) and AoA (right) at 90% blade span, MEXICO rotor, Wind speed = 15m/s with 30° yaw
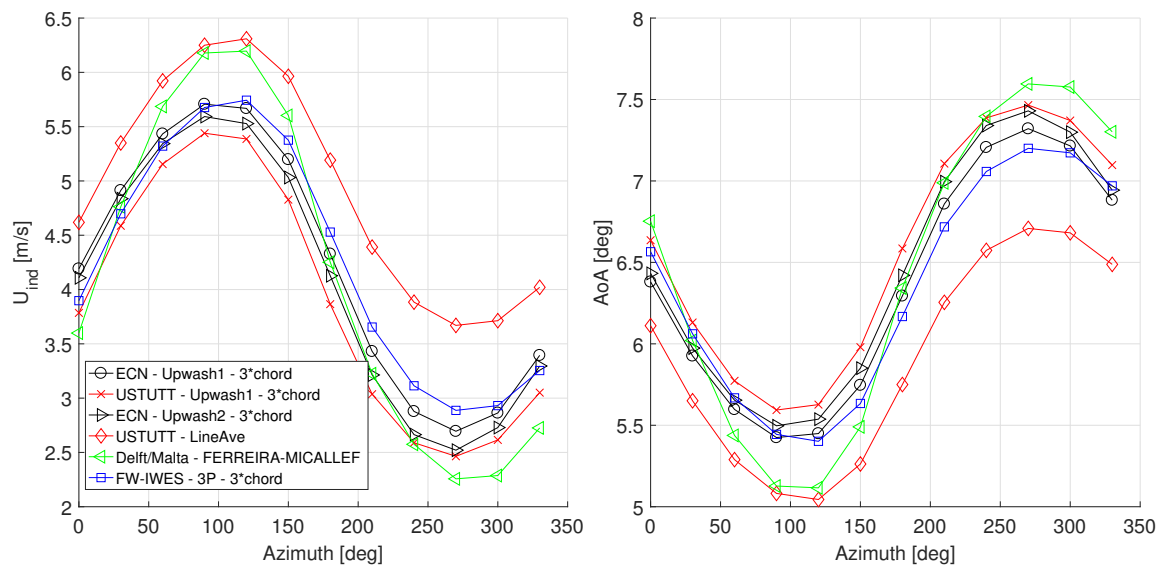
at circa 6°, thus within this large drag gradients the relative differences between the methods rapidly increases to circa 22% for azimuth > 150°, where the operating AoA > 6°.

5. Conclusion
While the calculation of the angle of attack remains an abstract concept in that it cannot be directly verified experimentally or numerically using full CFD, the presented results provide an exhaustive comparison of the various approaches that have been previously documented in the literature. For the first time, the angles of attack is calculated using variety of methods, in the case of a yawed turbine at various azimuthal location on the basis of full CFD calculations. The
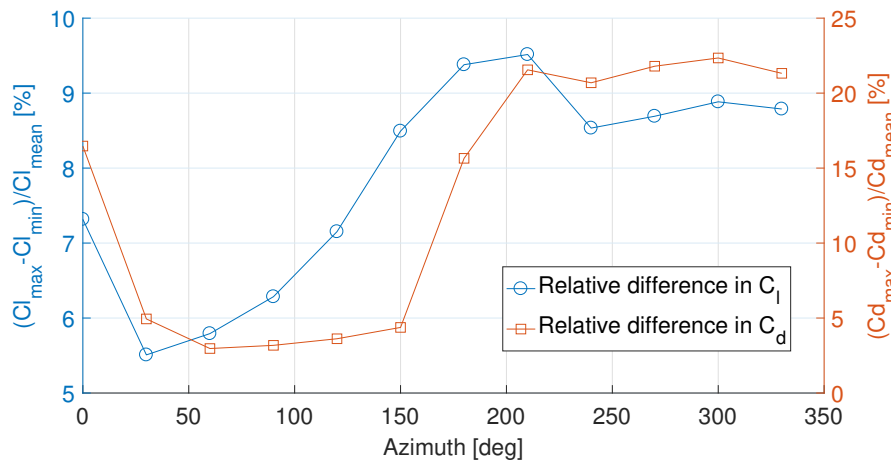
Figure 11. Relative differences in BEM force coefficients between all methods at 90% blade span

observed discrepancies between the methods are mostly found towards the root of the blade, where up to 70% difference is seen for the drag force. The reasons for this have been attributed to the influence of the root vortices and the highly three dimensional nature of the root flow which are for the most part unaccounted for by the presented models. This work cannot claim any particular method to be superior to the other in terms of predictive accuracy, however the presented comparison shows inadequate agreement between these methods for application towards the root.

All in all however, the agreement between the methods is fairly reasonable from mid and tip parts of the blade with differences in angle of attack of circa 1°. Despite the small differences in AoA, larger uncertainties are incurred if and when the interested section operates beyond the linear region and such differences can be important when considering the resulting airfoil loads, the qualitative agreement in the trends is encouraging.

Additionally, it can be still concluded that the yawed case does not uncover any particular flaw in the adopted approaches which would have made them unsuitable in this circumstance. Perhaps the only exception to this was found in the root region where the strong cross interactions between the wakes released by the individual blades can be problematic.

6. References

[1] Schepers J 2012 *Engineering models in wind energy aerodynamics, development, implementation and analysis using dedicated aerodynamic measurements* Ph.D. thesis University of Delft (*Preprint* `doi:10.4233/uuid:92123c07-cc12-4945-973f-103bd744ec87`)

[2] Rahimi H, Schepers J, Shen W, Garca N R, Schneider M, Micallef D, Ferreira C S, Jost E, Klein L and Herrez I 2018 (*Preprint* `Renewable Energy, arXiv:1709.04298`)

[3] Sørensen N N, Bechmann A, Réthoré P E and Zahle F 2014 *Wind Energy* **17** 75–86 ISSN 1099-1824 URL `http://dx.doi.org/10.1002/we.1559`

[4] D Micallef, CS Ferreira, T Sant G v B 2014 *Wind Energy* **17** 657–669 URL `http://onlinelibrary.wiley.com/doi/10.1002/we.1608/full`

[5] Haans W, van Kuik G and van Bussel G 2007 *Journal of Physics: Conference Series* **75** 10pp

[6] Tongchitpakdee C, Benjanirat S and Sankar L N 2005 *Journal of Solar Energy Engineering* **127** 464–474 ISSN 0199-6231 URL `http://dx.doi.org/10.1115/1.2035705`

[7] Rahimi H, Garcia A M, Stoevesandt B, Peinke J and Schepers J G 2018 *Wind Energy* ISSN 1099-1824 URL `https://doi.org/10.1002/we.2182`

[8]   Rahimi   H,   Dose   B,   Stoevesandt   B   and   Peinke   J   2016   **749**   012015   URL
       http://stacks.iop.org/1742-6596/749/i=1/a=012015

[9]   Schepers J G and Boorsma K 2012 *Final report of IEA Task 29 Mexnext (Phase 1): Analysis of Mexico wind
       tunnel measurements*

[10] Maeda T, Kamada Y, Suzuki J and Fujioka H *J. Sol. Energy Eng* **130** 31017–31018

[11] Micallef D 2012 *3D flows near a HAWT rotor : A dissection of blade and wake contributions* Ph.D. thesis

[12] Micallef D and Sant T 2016 A review of wind turbine yaw aerodynamics *Wind Turbines-Design, Control and
       Applications* (InTech)

[13] Del Campo V, Ragni D, Micallef D, Akay B, Diez J and Ferreira C 2013 Non intrusive 3D load calculation
       during yaw conditions *European Wind Energy Conference and Exhibition, EWEC 2013* vol 2 ISBN
       9781632663146

[14] del Campo V, Ragni D, Micallef D, Diez J and Ferreira C S 2014 *Wind Energy* **17** 657–669 URL
       http://onlinelibrary.wiley.com/doi/10.1002/we.1608/full

[15] Michelsen J A 1992 Basis3d-a platform for development of multiblock pde solvers Tech. rep. Technical Report
       AFM 92-05, Technical University of Denmark

[16] Michelsen J A 1994 *Block structured Multigrid solution of 2D and 3D elliptic PDE's* (Department of Fluid
       Mechanics, Technical University of Denmark)

[17] Sørensen N N 1995 *General purpose flow solver applied to flow over hills* Ph.D. thesis Risø National
       Laboratory

[18] Boorsma K and Schepers J 2015 Description of experimental setup, new mexico experiment. technical report
       Tech. Rep. ECN-X15-093 ECN

[19] WZ Shen M H and Srensen J 2007 Determination of angle of attack (aoa) for rotating blades. *In Proceedings
       of the Euromech Colloquium Wind Energy 2005. Peinke, Schaumann, Barth (eds)* (Springer, Berlin,
       Heidelberg. 205-209.)

[20] WZ Shen M H and Srensen J 2009 *Wind Energy* **12** 91–98

[21] Jost E, Klein L, Leipprand L, Lutz T and Kramer E 2017 Extracting the angle of attack on rotor blades
       from cfd simulations (*Preprint* Wind Energy, accepted for publication)

[22] Rahimi   H,   Hartvelt   M,   Peinke   J   and   Schepers   J   2016   **753**   022016   URL
       http://stacks.iop.org/1742-6596/753/i=2/a=022016

[23] Johansen J and Sørensen N N 2004 *Wind Energy* **7** 283–294

[24] Hansen M O, Sørensen N N, Sørensen J N and Michelsen J A 1998 Extraction of lift, drag and angle of
       attack from computed 3-d viscous flow around a rotating blade *1997 European Wind Energy Conference*
       (Irish Wind Energy Association) pp 499–502

[25] Vimalakanthan K 2014 *Passive flow control devices for a multi megawatt horizontal axis wind turbine* Ph.D.
       thesis Cranfield University (*Preprint* http://dspace.lib.cranfield.ac.uk/handle/1826/12132)